urban science

MDPI

Article

The Urban Archipelago Effect: A Case Study in Morocco

Lahouari Bounoua [1,*], Tao Zhang [2], Kurtis John Thome [1], Noura Ed-dahmany [3], Mohamed Amine Lachkham [3], Hicham Bahi [4], Mohammed Yacoubi Khebiza [3] and Mohammed Messouli [3]

[1] Biospheric Sciences Laboratory, National Aeronautics and Space Administration, Goddard Space Flight Center, Greenbelt, MD 20771, USA
[2] Department of Geological and Atmospheric Sciences, Iowa State University, Ames, IA 50011, USA
[3] Laboratory of Water Sciences, Microbial Biotechnologies, and Natural Resources Sustainability (AQUABIOTECH), Faculty of Sciences Semlalia, Cadi Ayyad University, Marrakesh 40000, Morocco; n.eddahmany.ced@uca.ac.ma (N.E.-d.); m.lachkham.ced@uca.ac.ma (M.A.L.); messouli@gmail.com (M.M.)
[4] African Research Center on Air Quality and Climate, Mohammed VI Polytechnic University, Ben Guerir 43150, Morocco
* Correspondence: lahouari.bounoua@nasa.gov

Abstract: We model and describe the combined effect of a series of urban heat islands (UHIs), generated by nearby cities aligned as an archipelago, on the vertical diffusion of heat and the temperature structure in the lower atmosphere over an urban chain in northwestern Morocco. We use the Weather and Forecasting Model (WRF) coupled to an urban canopy model to run simulations during the northern summer. We show that when the land surface is characterized accurately, the WRF model can effectively resolve the scale of the urban archipelago effect and describe its detailed diurnal structure. Our results indicate that the combined effect of multiple UHIs in proximity is more impactful than the sum of their parts. Specifically, the urban archipelago's effect alters the vertical temperature structure through upward diffusion of heat and extends its scale from local to meso-scale. This alters the wind pattern and may affect local weather conditions and air quality. These results underline the importance of considering the urban archipelago effect when studying urban climate. They also extend beyond academic research to offer valuable insights for urban planners in emphasizing the importance of urban typology and spatial proximity in city design and balancing cities' interconnectivity with sustainable development and resilience.

Keywords: urban archipelagos; urban heat island; lower atmosphere; WRF model; thermal structure; local climate

Academic Editor: Luis Hernández-Callejo

Received: 18 January 2025
Revised: 3 March 2025
Accepted: 19 March 2025
Published: 26 March 2025

Citation: Bounoua, L.; Zhang, T.; Thome, K.J.; Ed-dahmany, N.; Lachkham, M.A.; Bahi, H.; Yacoubi Khebiza, M.; Messouli, M. The Urban Archipelago Effect: A Case Study in Morocco. *Urban Sci.* **2025**, *9*, 97. https://doi.org/10.3390/urbansci9040097

1. Introduction

The world population reached 8 billion in 2022 [1] with more than half living in urban areas. This trend is continuously increasing, and despite the many efforts to stabilize rural population migration, more people are still moving to urban areas in search of higher income and better life standard, especially in emerging countries, where the migration of labor to urban areas is an important part of the urbanization process [2]. Urban areas are formed of dense artificial structures such as houses, schools, commercial buildings, roads, and parking spaces. These structures alter the surface energy balance and, consequently, the surface climate in ways that are not entirely understood, and the extent of their impact on local and regional temperature and weather patterns has not been extensively evaluated.

In emerging countries, urbanization is having an even greater impact as more people seek better life and social services in cities. For example, North Africa is an urbanization

hot spot where 78 percent of the population lives in cities, making it one of Africa's most urbanized regions. Indeed, between 2000 and 2015, the level of urbanization increased by around 1.5 percent in North Africa making it the fastest growing region after East Africa [3]. More important is that most of this urbanization is happening along a narrow coastal strip of arable lands constrained between the Sahara to the south, the Mediterranean Sea to the north and the Atlantic Ocean to the west, resulting in relatively large cities with high urban density along the coastline forming an archipelago shape (Figure 1). By 2022 in Morocco, the focus area of this study, nearly 65 percent of the total population lived in urban areas where natural lands have been converted to artificial impervious structures [4].

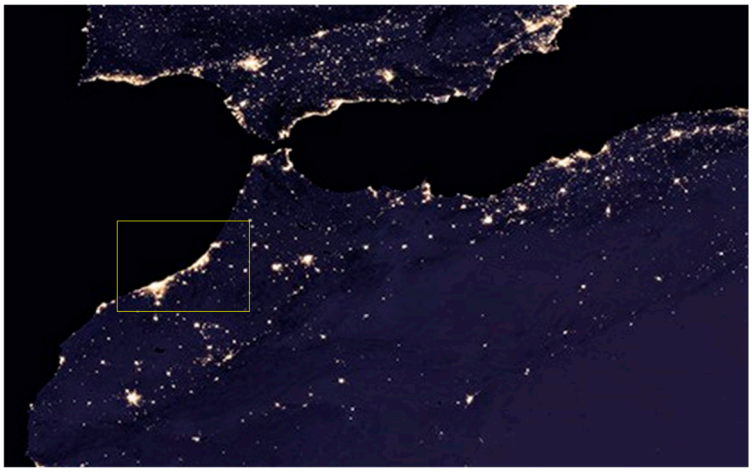

Figure 1. Northwestern African cities as seen by night. The yellow box limits the urban archipelago of interest, generated by the two metropoles of Casablanca and Rabat. Courtesy of the NASA Earth Observatory (2016).

Ref. [5] addressed the impact of urbanization on surface climate and showed that urban buildup affects the surface climate through several distinct physical mechanisms, the most important of which was a lower albedo and the distribution of absorbed incoming solar energy between latent and sensible heat fluxes. The study provided a detailed analysis of the impact of urban buildup on the surface (skin) temperature structure as well as on the surface runoff and the carbon sequestration lost to urbanization over the continental United States (CONUS). Defining the urban heat island (UHI) and the urban heat sink (UHS) as the positive and negative temperature difference between the urban and rural zones, respectively, the study concluded that in cities built within forested or otherwise vegetated lands, daytime urban surface (skin) temperature was much warmer than that of the surroundings, thus creating a well-defined UHI. Conversely, in cities built within semi-arid lands, temperature was cooler than that of surrounding shrubs, forming a UHS. On average, during the boreal summer, the study showed that over the CONUS, cities were 1.9 °C warmer than surrounding vegetated lands.

Other studies have also addressed urbanization, and most of them focused on the UHI and its amplitude [6]. The UHI is a well-known phenomenon resulting from the differential heat absorption properties of urban buildup material as compared to surrounding rural natural lands. Using satellite data over 38 of the most populous urban centers of the continental US, [7] found that the annual average temperature in urban areas is 2.9 °C warmer than that of the surrounding non-urban fringe. In Europe, [8] investigated the UHI intensity and its spatial distribution across several European cities and found significant differences influenced by population density, land use patterns, and climate conditions and suggested that sustainable urban development and climate-resilient spatial planning play an important role for climate change adaptation in urban areas. On the other hand, [9]

used satellite data to explore the influence of urban density and shape on the UHIs in the northeast United States and showed that for cities of similar sizes, the impervious surface density distribution within the city and its shape as measured by the area to perimeter ratio are significant factors influencing the UHI magnitude.

In Morocco, [10] suggested a monotonic increase in UHI amplitude with urban area size. They also showed that, as urban areas built in desert-like environments grow, the UHS amplitude gradually decreases to ultimately turn into a UHI. More importantly, they assessed the impact of land use on the UHI and UHS over several Moroccan cities based on local climate zoning, size, and typology during a northern summer. Typically, their results showed multiple causes defining the different shapes and amplitudes of the UHI, namely the ambient climate, the proximity to the sea, the presence of landscaped areas, and the color of building material. Furthermore, they showed that at the neighborhood level, local urban aggregate or towns are usually cooler than surroundings, invoking irrigated vegetation within towns as a cause for the relative cooling. On a local scale, [11] carried out a study to highlight and monitor the spatial and seasonal distribution of surface UHI in the Casablanca region.

While these studies provided insights on the UHI's horizontal structure and its amplitude, none of the studies examined its effect on the vertical temperature structure and its interaction with lower atmospheric circulation and local weather. The authors of [12] were among the researchers who analyzed rain gauge data to quantify the effect of urbanization of the Houston (TX, USA) urban area on the local diurnal rainfall pattern. They compared rainfall from two periods centered circa 1950 when Houston was relatively small with no significant impact on weather patterns and around 1990 when it grew up to become a major metropolitan area. They found that during an average warm season from 1984 to 1999, the urban area and downwind urban-impacted region registered 59% and 30%, respectively, greater rainfall than an upwind control region, with most of this increase recorded during the afternoon and through the night. This suggests that the effects of urbanization on the atmosphere extend into the planetary boundary layer (PBL) and go beyond affecting surface air temperature to alter the PBL air circulation, clouds, and precipitation.

This study is based on the findings of Burian and Shepherd (2005) [12] and follows along the path of the urban archipelagos effect proposed by [13]. The primary goal of this paper is to model and assess the impact of UHIs generated by a series of nearby cities in the Northwestern coast of Morocco, aligned as an archipelago on the vertical diffusion of sensible heat and the temperature structure in the lower atmosphere. UHIs are micro scale phenomena, and their combination is a challenge to parameterize in an Earth system model framework. Our methodology uses an advanced model including an urban canopy sub-model based on explicit parameterization of surface fluxes. The model reproduces the sub-scale phenomenon and predicts its diurnal evolution at an hourly timeframe, which should be beneficial for urban planning and heat mitigation in urban areas.

2. Data, Model, and Method

2.1. Data

The Global Forecast System analysis of weather data from 1 August and 4 August 2014, available at the National Oceanic and Atmosphere Administration (NOAA) National Centers for Environmental Information (NCEI) (https://www.ncei.noaa.gov/has/HAS.DsSelect (accessed on 15 November 2023)), was used to describe the Weather Research and Forecasting (WRF) model's initial and lateral boundary conditions. The spatial resolution is 0.5 degrees, and the temporal resolution is 6 h.

WRF Preprocessing System (WPS) geospatial input data were downloaded from the WRF official website (https://www2.mmm.ucar.edu/wrf/users/download/get_sources_

wps_geog.html (accessed on 15 November 2023)) to initialize the WRF model. To improve the model's performance, impervious surface area (ISA) data and land cover (LC) data were used to update corresponding variables in the default WRF model. The 2014 ISA data at a 1 km resolution was used to characterize the urban areas in the WRF model. The ISA was aggregated from the original Global Artificial Impervious Area (GAIA) dataset at 30 m resolution for the same year. The original GAIA ISA data were mapped with Google Earth Engine using the full archive of 30 m resolution Landsat images from 1985 to 2018, reaching a mean overall accuracy higher than 90% [14].

The land cover (LC) data at 500 m resolution in 2014 were used to update the default LC in the WRF model. The original LC data were extracted from the MODIS Land Cover Dynamics Version 6.1 (MCD12Q2 v061) yearly land surface phenology metrics data product at 500 m resolution (https://lpdaac.usgs.gov/products/mcd12q2v061/ (accessed on 11 December 2023)). Then, the World Settlement Footprint (WSF) Evolution (1985–2015) dataset with a spatial resolution of 30 m, which was derived through multitemporal Landsat-5 and Landsat-7 imagery [15,16], was used to refine the MODIS LC data in this study. We labeled each pixel in the 500 m resolution MODIS LC data as 'urban and built-up', when the overlapped 30 m resolution pixels of the WSF in 2014 are dominated by urban settlements. This is because the WSF data are at a higher resolution and are more accurate than the MODIS LC 'urban and built-up' data.

2.2. Model

The WRF Model coupled with the Urban Canopy Module (WRF/UCM) version 4.1, which has been widely used for modeling urban climate [17–19], was employed in this study. WRF is an advanced numerical weather prediction system developed by the US National Center for Atmospheric Research (NCAR) to study urban systems; an integrated urban modeling module was developed to couple with the Noah land surface model (Noah-LSM) scheme of WRF [20]. Meanwhile, Noah-LSM was coupled with the single-layer urban canopy model (SLUCM), which considers factors such as the reflections, shadowing, and trapping of radiation, the street orientation and diurnal variation of the azimuth angle, the surface energy budget of roofs, walls, and roads, the wind profile in the canopy layer, and anthropogenic heat emissions [18,21]. The WRF model is designed for both atmospheric research and operational forecasting. It is highly versatile, capable of simulating a wide range of atmospheric phenomena from regional-scale weather patterns to local-scale features like thunderstorms and turbulence. WRF is widely used by meteorologists, researchers, and operational forecasters worldwide due to its flexibility and scalability. A comprehensive description of the WRF model can be found in [22].

2.3. Method

To assess the effects of surface UHIs created by a chain of aligned cities on the vertical temperature and wind fields' structure, a series of high-resolution numerical simulations using the WRF-model was conducted over a coastal region in northwestern Morocco presenting a chain of cities in proximity along the axis of Casablanca, Mohammedia, and Rabat (Figure 2). The simulations were carried out during summertime from 1 August to 4 August 2014, over three nested domains designed in the study area with a horizontal grid spacing of 15 km (D1), 3 km (D2), and 1 km (D3), respectively (Figure 2A). The period of study was selected to represent a typical summer period with stable atmospheric conditions, high urban heat intensity, and minimal synoptic disturbances, allowing for a clear assessment of the urban archipelago effect. While this study focuses on summer conditions, it is important that future work explores inter-seasonal variations and assesses the behavior of the urban archipelago effect across different climatic conditions. The first

24 h of simulations were used for spin-up time, and the outputs were recorded at 3 h, 3 h, and 1 h intervals for domains D1, D2, and D3, respectively. The simulation results from domain D3 with the finest resolution are used for analysis in this study.

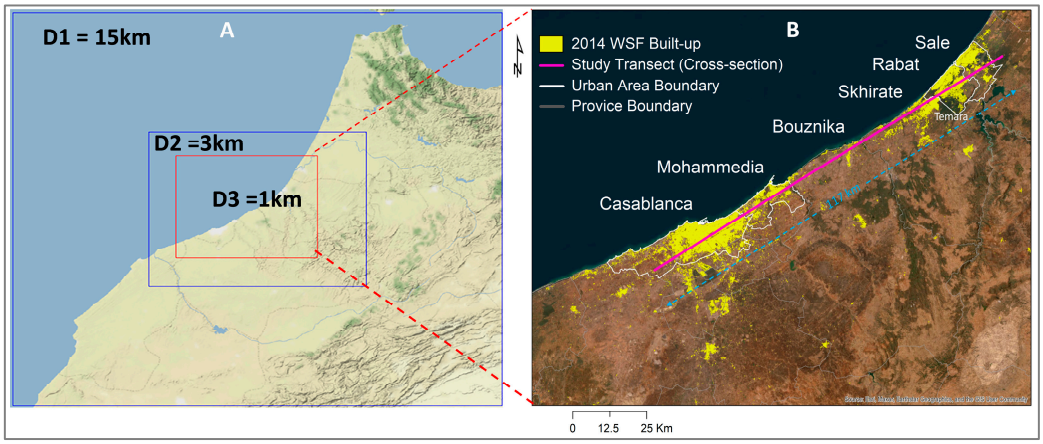

Figure 2. (**A**) Model domains with multiple resolutions: D1 with 15 km, D2 with 3 km, and D3 with 1 km spatial resolution; (**B**) cities' alignment in the inner domain. Red line is a transect across cities where the temperature vertical structure is being analyzed.

3. Results and Discussion

3.1. The Urban Heat Island

Urban heat islands (UHIs) are localized zones of elevated temperatures in urban areas compared to their surrounding rural environments [7,23,24]. This phenomenon arises from the altered energy balance at the Earth's surface due to urbanization, where natural landscapes are replaced with impervious materials like concrete, asphalt, and buildings. These materials have high thermal capacities and low albedo, absorbing and retaining more solar radiation. The replacement of vegetation also reduces evapotranspiration, a key cooling process in natural systems, leading to a shift in energy partitioning. As a result, the sensible heat flux—the transfer of heat from the surface to the atmosphere—dominates over latent heat flux, creating warmer urban lower atmospheres and rising motion.

The UHI effect, a sub-grid phenomenon that is challenging to capture with coarse observation networks, can be evidenced through the analysis of dry static energy (DSE), a key physical quantity in atmospheric thermodynamics. DSE is the sum of the internal energy of air, proportional to its temperature, and the potential energy associated with its height in the atmosphere. In urban areas, excess sensible heat flux caused by a lack of latent heat release at the surface leads to an increase in air temperature, thereby raising the thermal component of DSE. This localized increase in DSE creates a buoyancy effect, as warmer, less dense air tends to rise above cooler surrounding air. These heat exchange processes occur at spatial scales smaller than the grid size of the model and, therefore, are not explicitly resolved but rather apparent to the large-scale dynamics driving the urban heat island. These exchanges can be formalized by considering the change in DSE forced by surface diabatic heating within the city and its impact on large scale motion.

$$\frac{dS}{dt} = Q_r + L(c - e) \tag{1}$$

where $S = C_pT + gz$ is the DSE, T is the temperature, C_p is the specific heat at constant pressure for dry air, z is the height, and g is the acceleration of gravity. Q_r is the radiative heating rate and the term $L(c - e)$ represents the net condensation heating, which in this

dry adiabatic process is null. Since z is constant, the change in S is entirely due to a change in temperature, and for dry adiabatic processes S is conserved, therefore

$$\frac{dS}{dt} = 0 \tag{2}$$

The right-hand side of (1) represents the forcing which drives the total change in S and shows that, in the absence of net condensation, the surface heating in the city is entirely radiative.

Using the perturbation theory, whereby a quantity can be expressed by an area average value and a deviation from it, it can be shown that (1) may take the following form:

$$\frac{\partial \overline{S}}{\partial t} + \overline{V.\nabla S} + \overline{\omega}\frac{\partial \overline{S}}{\partial p} = Q_r + L(c-e) - \frac{\partial \overline{(s'\omega')}}{\partial p} \tag{3}$$

where the bar terms represent the area averages, and the primes represent their deviations. The first term in the left-hand side of (3) is the local variation of the area average S, and the second and third terms represent its horizontal and vertical advection, respectively. The last term on the right-hand side is the convergence of the turbulent heat flux. Following [25], the sub-grid heat apparent to the large-scale is expressed as

$$Q_1 = Q_r + L(c-e) - \frac{\partial\left(\overline{s'\omega'}\right)}{\partial p} \tag{4}$$

Integrating (4) from a pressure level at which eddies vanish (pt) to the surface (ps) gives

$$\frac{1}{g}\int_{pt}^{ps}(Q_1 - Q_r)dp = \frac{L}{g}\int_{pt}^{ps}(c-e)dp - \frac{1}{g}\left(\overline{s'\omega'}\right)_{p=ps} \tag{5}$$

Because there is no net condensation, (5) reduces to

$$\frac{1}{g}\int_{pt}^{ps}(Q_1 - Q_r)dp = -\frac{C_p}{g}\left(\overline{T'\omega'}\right)_{p=ps} \tag{6}$$

where $-\frac{C_p}{g}\left(\overline{T\prime\omega\prime}\right)_{p=ps}$ is the vertical eddy transport of sensible heat flux. Equation (6) indicates that the apparent heating Q_1 of the large-scale motion consists of the radiative heating and the vertical eddy transport of sensible heat. In other words, the sub-grid heat generated by solar radiation in urban areas is transferred to the atmosphere via vertical eddies which create turbulent vertical motions and affect the vertical temperature structure, thus forming the urban heat dome. Equations (1)–(6) establish the theoretical framework linking sub-grid heating processes to the large-scale dynamics driving the urban archipelago effect.

3.2. Simulated Results

In this study, the situation is more complex as we analyze a combination of UHIs resulting from a series of urban centers forming an urban archipelago along the western coast of Morocco (Figure 2B). The study region is characterized by an oceanic climate maintaining relatively mild temperatures throughout the year with refreshing summer sea breezes. In the Casablanca-Rabat region, the climatological maximum temperature typically reaches around 26 °C during the summer months, while the minimum temperature in winter averages around 10 °C, with occasional dips below that point; overall, the region experiences dry summers and damp winters. There, local vegetation is adapted to summertime temperatures and its transpiration keeps the city relatively cooler than the

concrete and asphalt of the urban tissue. This effect is more evident in Casablanca than in Mohammedia.

The UHI generated by the three cities of Casablanca, Mohammedia, and Rabat is shown in Figure 3B. To obtain the surface temperature data used in this graphic, we select a quadrant defined by axes passing through the three cities and including the largest part of the urban areas (Figure 3A). The temperature profile is then obtained by averaging temperatures from all grid points included within the quadrant, except for water. The simulated impact of urban buildup on surface air temperature is illustrated along the quadrant including the three cities (Figure 3B). It is represented by the difference between the average skin temperature weighted by the fractions of all land cover co-existing in the grid and the weighted average temperature of the vegetation only, respectively, represented by "Act temp" and "Veg temp" in Figure 3B. Across the cities, this difference clearly shows the impact of the buildup on the city's skin temperature. This impact is on the order of 0.5 °C in Casablanca and about 0.2 °C in Mohammedia; further northeast along the transect, in the city of Rabat, the impact of the buildup on skin temperature is 0.4 °C.

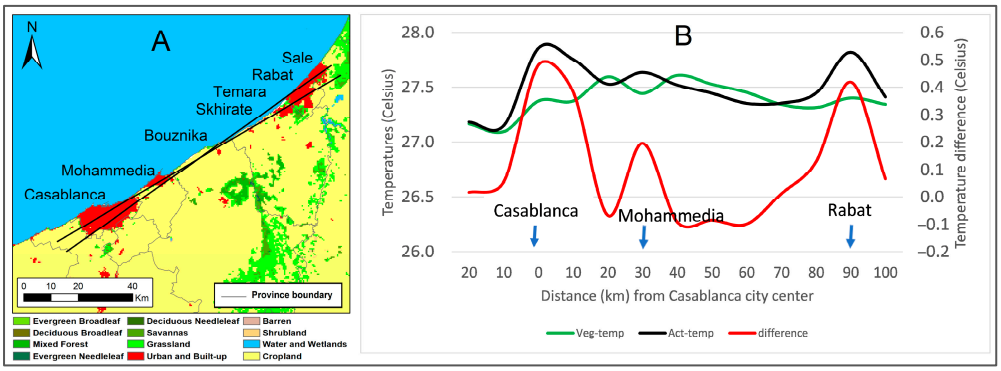

Figure 3. Mean temperature profile across the cities Casablanca, Mohammedia, and Rabat. Panel (**A**) shows the land cover map and the southwest to northeast axes defining the quadrant where temperature was averaged to construct the profile. Panel (**B**) shows the actual (black) and vegetation-weighted (green) skin temperatures. Their difference (actual minus vegetation) is shown in red.

The amplitude of this difference appears to be related to the size of the urban area. This contrast in temperature between urban and non-urban areas and its relation to the city-size is like the relationship between the UHI and population size reported in [26]. This impact is different from the UHI and represents the increase in temperature generated by the buildup material within the city. Indeed, the stretch of buildup between Casablanca and Mohammedia reveals a dense mosaic of development. As these towns seamlessly merge into one another, the landscape transitions from bustling cityscapes to quieter suburban enclaves, reflecting a gradient of urban density. Like Casablanca but smaller in size, Rabat shows similar patterns and in dense urban areas, the prevalence of heat absorption contrasts with the cooling effects of surrounding vegetation. These urban environments, characterized by large areas of concrete, asphalt, and buildings, exhibit a strong surface urban heat island (SUHI). To show that, we choose the city of Casablanca and define its center based on the density of the impervious surface. A buffer zone is then defined around the city center extending outward to the city limits, and a series of axes connecting the city center to the buffer edge is used to capture the temperature within the defined quadrant (Figure 4A). This is an extreme case where the city temperature contrasts with that of the ocean with an amplitude exceeding 5 °C (Figure 4B). On the other side, in the southeast quadrant, where the landscape is characterized by fallow land, the skin temperature gets warmer than that of the city center. This local warming in cities is exclusively due to impervious surfaces which differentially absorb and retain solar radiation and may be

amplified by the heat generated by anthropogenic activities and exacerbated by climate warming [27]. The heat dome over the city generates local turbulent eddies which transport the heat upward and affect the temperature vertical structure.

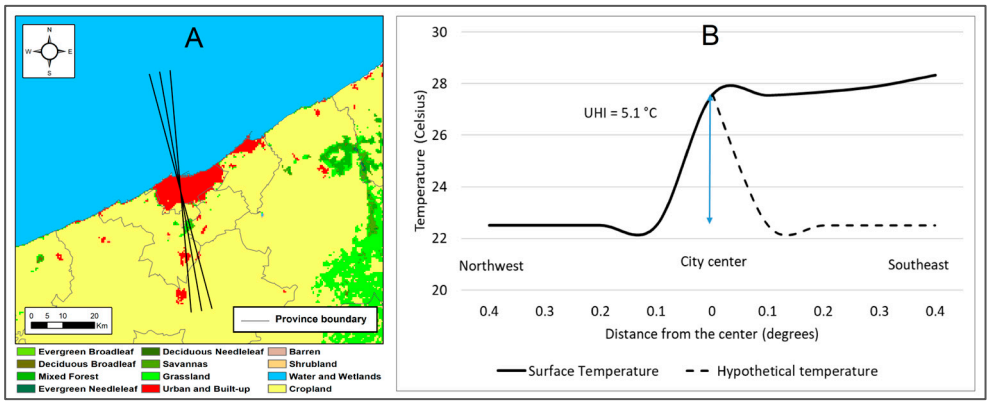

Figure 4. Mean temperature profile across Casablanca. Panel (**A**) shows the land cover map and the selected northwest–southeast axes defining the quadrant where temperature was averaged to construct the cross section. Panel (**B**) shows the surface skin temperature profile along the northwest–southeast quadrant across Casablanca. The dashed line represents a hypothetical temperature profile obtained by symmetry with respect to the city center.

Our model simulations started on 1 August 2014 at 00 a.m. and were integrated forward in time for 96 h over domain D3 shown in Figure 2A. The initial conditions show a thermal stratification in which, at an elevation of about 1 km, a layer of warm air reminiscent of the previous day's heating is centered at about 1.5 km and extends to about 2.25 km in height. Underneath it is a layer of cooler air overlaying a stable surface of relatively warm air confined to the lowest 500 m with a near surface air temperature of 291 K extending all along the transect between Casablanca and Rabat (Figure 5). By 6 a.m., the surface air temperature has decreased to 290 K over all the urban areas along the transect. However, at 12 a.m., clear heat domes are simulated over the regions of Casablanca and Rabat urban areas with surface air temperatures reaching 295 K and 294 K, respectively. The heat generated over Casablanca is advected by a southwest sea breeze along the coast all the way to Rabat about 90 km northeast. The heat dome over Rabat is further intensified by warm southwest air from the towns of Skhirate and Temara (see Figure 2B). There is a generalized upward conduction of heat all along the transect from the surface to about 1 km. Over the Rabat agglomeration, however, the heat dome has intensified and turned into a plume of eddy vertical heat transport that pierced the lower surface layer to a height of 1.5 km where it formed an anvil (Figure 6). At the surface, all along the transect over the archipelago of cities (Casablanca, Mohammedia, Bouznika, Skhirate, Temara, and Rabat), the first 1 km of the boundary layer has warmed significantly to reach the seasonal average temperature of about 295 K, and by 3 p.m. local time, when the insolation and temperature have reached their maxima, the temperature structure clearly shows the vertical diffusion of heat from the surface with two plumes, in the form of clouds, of heat established over the urban areas of Casablanca and Rabat, extending up to 1.5 km in height where they form anvils at the level of divergent flow and relatively cooler air. This illustrates how thermal and mechanical turbulence combine at the surface to upwardly transport the heat from the domes created over the urban areas (Figure 7). Between 3 and 5 p.m., the anvil over Casablanca dissipates gradually to completely disappear by 4 p.m., while that over the urban area of Rabat persists and still maintains its vertical structure. This is most likely due to the southwest breeze which cuts off the vertical heat diffusion over Casablanca and advects the surface heat towards the region of Rabat. By 6 p.m., the planetary boundary

layer (PBL) below 1 km has regained its thermal stratification from 295 K at the surface to 289 K at 1 km. However, the heat anvils over the two urban areas have merged to create a larger but cooler one covering the entire transect from Casablanca to Rabat. By this time, the sea breeze has completely cut off the vertical transport over Casablanca and has significantly diminished it over Rabat (Figure 8). During the first part of the night just after sunset, a net cooling of the surface boundary layer is observed with the 289 K isotherm dropping from about 900 m at 6 p.m. to 600 m at 9 p.m. At that time, the land surface air temperature becomes slightly cooler than the sea surface temperature and generates a land breeze which cools and stabilizes the lower boundary layer. By 9 p.m., the land–ocean temperature contrast has weakened, and the relatively warm air is confined to the first 600 m above the surface (Figure 9).

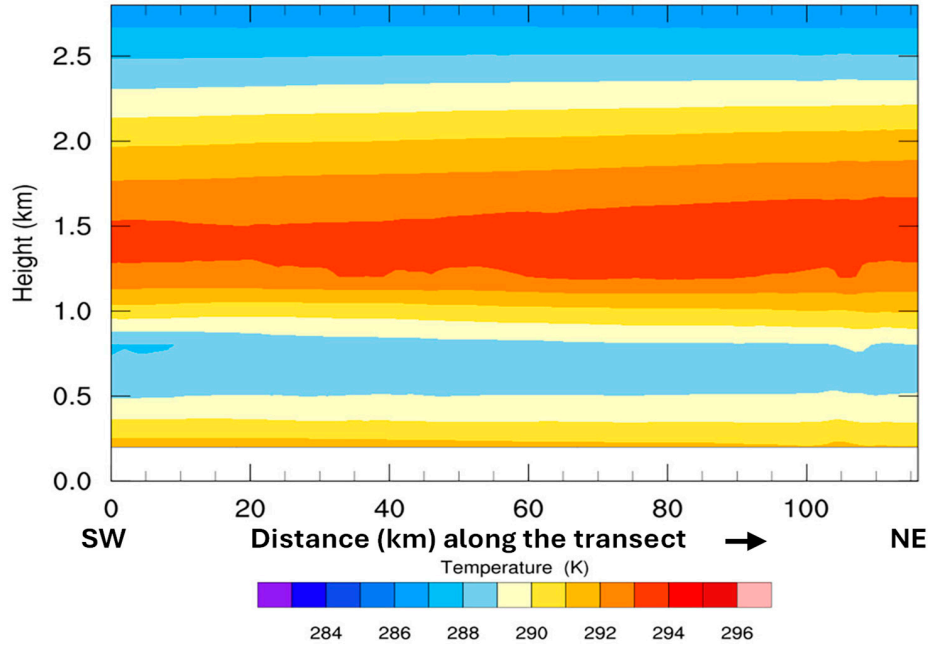

Figure 5. Model initial conditions valid on 1 August 2014 at 00.00 UTC.

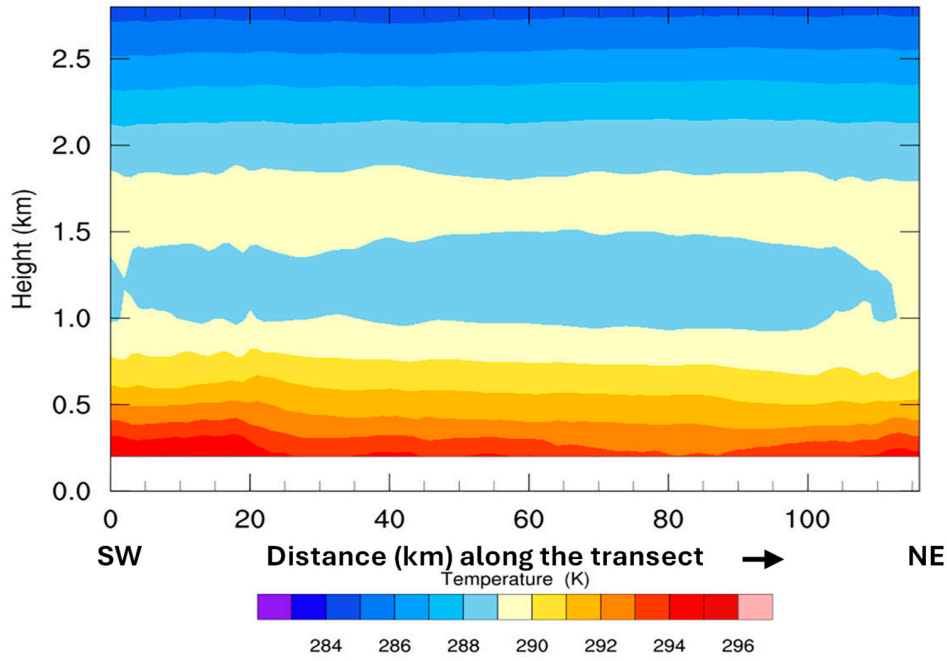

Figure 6. Simulated temperature for 1 August 2014 at 12.00 UTC.

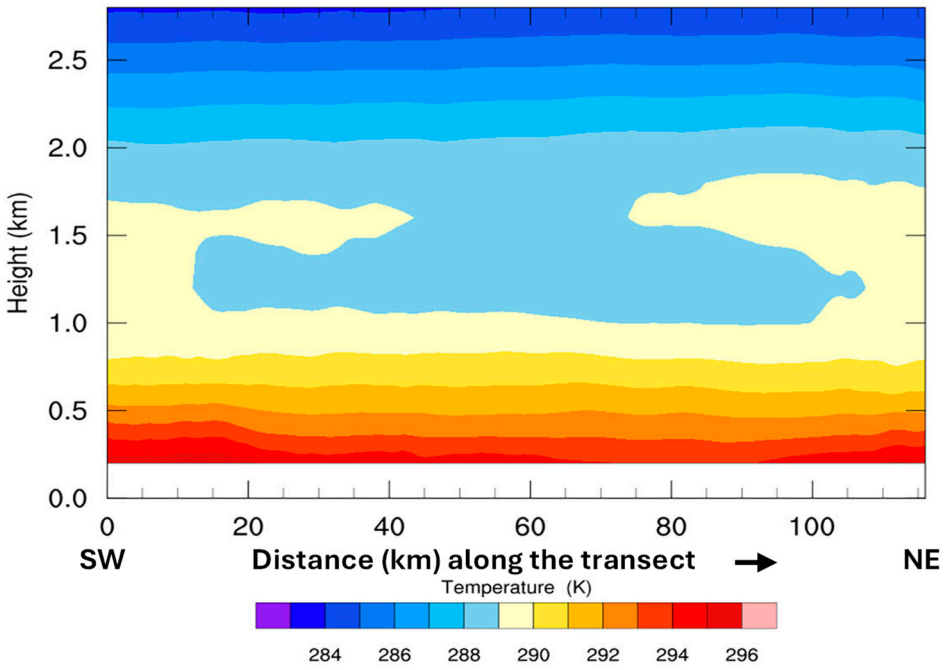

Figure 7. Same as Figure 6, except for 1 August 2014 at 15.00 UTC.

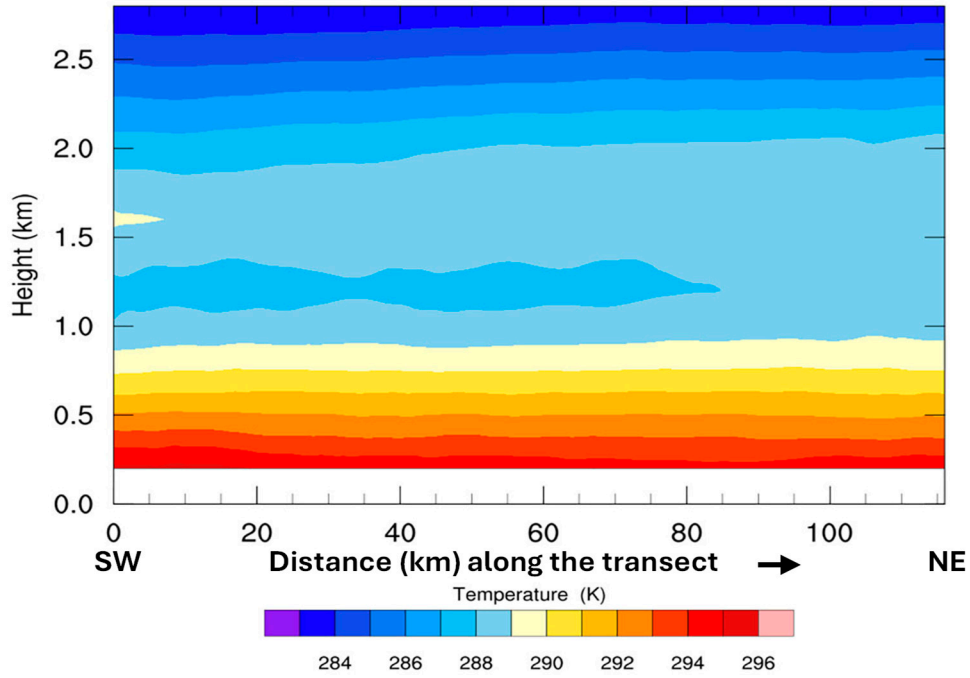

Figure 8. Same as Figure 6, except for 1 August 2014 at 18.00 UTC.

This cycle was basically repeated during the following three days with a surface air temperature warming to 296 K at 3 p.m. during the fourth day of the simulation, and where the PBL over the transect formed a huge plume of heat pushing the 289 K isotherm above 2.5 km. While the excess heating during the third and fourth day of simulations may not be directly associated with local conditions, its vertical distribution over the transect is the direct response of the archipelago of heat islands generated by the succession of cities along the transect. The interactions between the vertical transport of heat and the horizontal sea breeze circulation are illustrated in Figure 10 which shows the surge of relatively cool air with the 291 K isotherm penetrating inland at around 500 m and is more evident over the western part of the transect (Figure 10A). This surge is caused by the horizontal wind

blowing oceanic cooler air across the transect at about 500 m, showing a large part of its western side covered by the 291 K isotherm (Figure 10B).

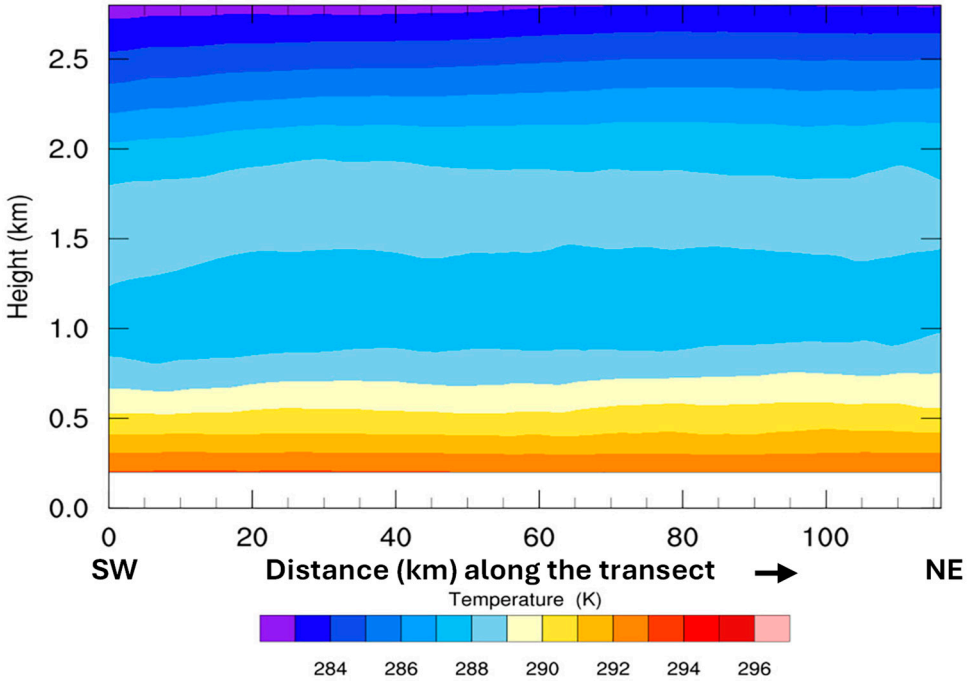

Figure 9. Same as Figure 6, except for 1 August 2014 at 21:00 UTC.

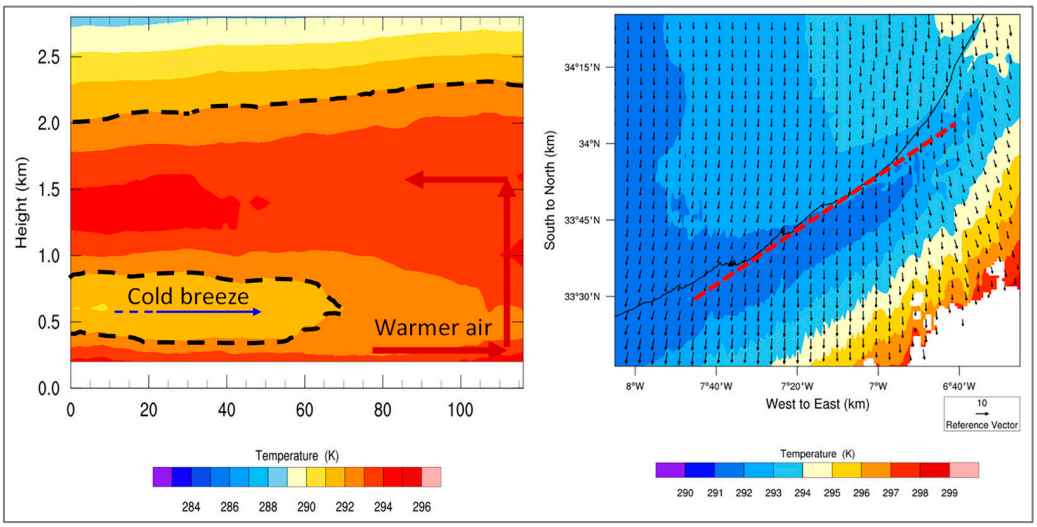

(**A**) (**B**)

Figure 10. (**A**) Simulated temperature cross section; dashed contour illustrates the penetration of cool breeze inland (blue line), and the red arrow indicates the vertical diffusion of heat. Panel (**B**) shows the horizontal wind and temperature at 500 m. The red dashed line shows the position of the transect and the black solid line indicates the coastline boundary. Figures in Panels (**A**,**B**) are valid 3 August 2014 at 17:00 UTC.

This phenomenon is relatively little known yet impactful, and its modeling has not been sufficiently documented. It is even more difficult to observe or measure it on the ground as it happens mostly in dry conditions and at small scales. In this research, we not only show that it is possible to model the effect created by multiple heat islands in proximity, but we also show that for the case of the transect between Casablanca and Rabat, the cumulative heat from the multiple heat domes increases the air temperature

in the lower atmosphere over the region, altering vertical temperature gradients and atmospheric stability. In the presence of moisture, the altered atmospheric conditions may affect cloud formation, convective processes, and precipitation patterns, which may lead to changes in rainfall intensity, distribution, and frequency. As an example, the Metropolitan Meteorological Experiment (METROMEX) conducted in St. Louis, MO (USA), was a comprehensive study that focused on understanding the effect of urban environments on weather patterns, particularly rainfall and storms. It was found that major cities could significantly modify local weather, leading to increased precipitation during the summer months. In fact, increased precipitation was observed both within the city and extending 50 to 75 km downwind, with rainfall increases ranging from 5 to 25 percent. The study results also indicated that the size of a city could influence the extent of its impact on rainfall [28].

The impact of the UHI effect on the vertical temperature structure has also been discussed by [29] over the large region of Beijing, revealing changes in temperature inversion layers and in the UHI circulation. The findings underscore the UHI effect's role in modifying local atmospheric conditions. A similar and more pronounced UHI effect on temperature inversion and its implications for air quality and weather patterns has also been suggested by [18]. In our study area, the proximity to the ocean creates a strong coupling between the urban heat vertical transfer and the sea breeze. While both phenomena are local in scales, their interaction affects the lower troposphere stability and may alter large scale weather patterns (Figure 11).

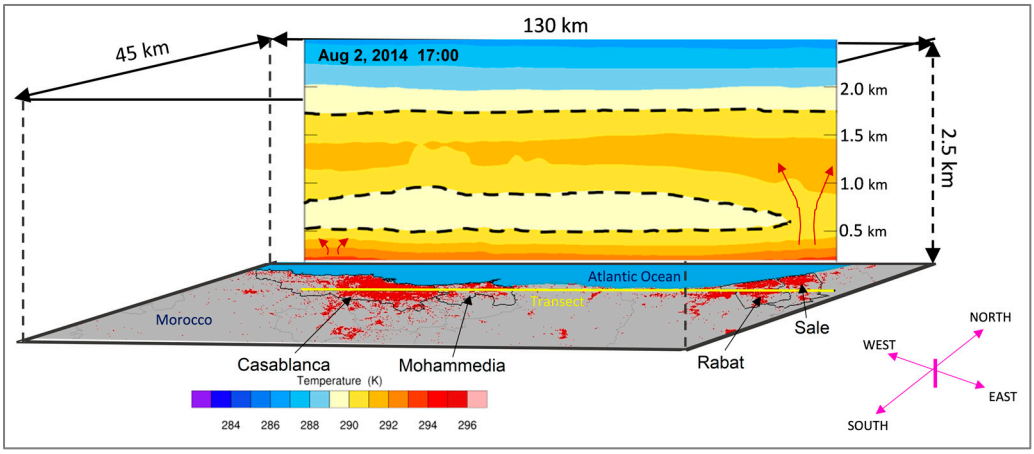

Figure 11. Schematic illustration of the interaction between the UHI archipelago and the sea breeze. The red arrows indicate the vertical diffusion of heat from the surface penetrating into the lower atmospheric boundary layer (dashed contour).

While this study provides valuable insights into the impacts of the urban archipelago effect on the lower boundary layer temperature structure and heat diffusion in a Mediterranean climate during summer, the findings may vary significantly under different seasonal or climatic conditions. For instance, winter scenarios, characterized by different atmospheric stability and moisture availability, could lead to distinct interactions between urban heat sources and boundary layer dynamics. Future research should explore these seasonal variations and conduct case studies in contrasting climates to comprehensively understand the broader implications of the archipelago effect on atmospheric processes.

4. Concluding Remarks

The urban archipelago effect, a phenomenon arising from the interaction of multiple urban heat islands (UHIs) in proximity, presents a significant challenge for understanding

and predicting its impact on the lower atmosphere. Existing studies, such as Zhao et al. (2019) [30], have primarily focused on quantifying UHI intensity and spatial patterns. However, these studies often overlook the potential for complex interactions between urban areas and surrounding environments, which may lead to the creation of heat "archipelagos" rather than continuous heat zones. In contrast, the "Urban Archipelago" concept provides a more nuanced understanding by recognizing the heterogeneous and dynamic nature of UHI distribution, offering insights into how urban development can create spatially distinct UHI clusters that vary in intensity and form over time. This approach adds a new layer of complexity to UHI studies by considering how urban form and geography contribute to the creation of heat islands that are not only localized but also interconnected in ways that traditional clustering methods may not capture and contextualizes the novelty of the urban archipelago concept.

Our study employed high-resolution numerical simulations to capture the time evolution of a series of UHIs generated by multiple cities located along the western coast of Morocco. These simulations have shown that when the land surface is accurately characterized, contemporary mesoscale models, like the WRF used in this study, can effectively resolve the urban archipelago effect scale and describe its overall impact at fine temporal resolutions. Indeed, the detailed representation of urban surfaces, including buildings, roads, and vegetation, is essential for capturing the nuances of UHI interactions.

Our results indicate that the combined influence of multiple UHIs can be more impactful than the sum of its individual components. This amplification arises from the interactions between the different heat islands, which leads to large-scale changes in the thermal structure and stability of the lower atmosphere. Specifically, we observed that the urban archipelago effect can lead to higher temperatures and altered wind patterns, which may in turn affect local weather conditions and air quality. These findings underscore the importance of considering the cumulative impacts of urban areas when studying urban climate.

The implications of our findings extend beyond academic research, offering valuable insights into urban planning and policymaking. Understanding the urban archipelago effect can inform strategies that emphasize the importance of spatial proximity and urban form in city design. While the arrangement and connections between urban clusters can be desired for economic activity and social interactions, our study provides crucial insights into how cities can be better designed and arranged to optimize these connections and still balance resilience and sustainable urban development. By incorporating these insights into urban design, cities can develop more effective measures to enhance mitigation of climate change and improve the quality of life for their inhabitants.

While the current study successfully demonstrates the ability of mesoscale models to simulate the archipelago effect when land surface characteristics are appropriately represented, we acknowledge that additional sensitivity studies, such as selectively removing cities, could further enhance our understanding of the phenomenon. These analyses would provide a deeper exploration of the relative contribution of individual urban areas to the simulated archipelago effect. Further, certain limitations should be acknowledged. The accuracy of WRF simulations relies on land use data, which may not fully reflect recent urban expansion. Incorporating higher-resolution datasets in future studies could improve precision. Additionally, the choice of WRF parameterization schemes may influence results; a sensitivity analysis would help assess potential variations. Lastly, as the study focuses on a short summer period with stable weather, examining different synoptic conditions and seasons would enhance the generalizability of the findings.

This research provides a comprehensive assessment of the urban archipelago effect, demonstrating that its impact on the lower atmosphere is significant and complex. The

ability of modern mesoscale models to resolve this effect, when coupled with accurate land surface characterization, offers a powerful tool for understanding and mitigating the environmental challenges posed by urbanization, especially within a changing climate. Future research should continue to refine these models and explore the long-term implications of the urban archipelago effects in the context of global climate.

Author Contributions: Conceptualization, L.B., K.J.T., N.E.-d. and M.A.L.; Methodology, L.B., T.Z., K.J.T., N.E.-d. and M.A.L.; Software, L.B. and T.Z.; Validation, L.B., K.J.T., T.Z., N.E.-d., M.A.L., H.B., M.Y.K. and M.M.; Formal analysis, L.B., T.Z., N.E.-d. and M.A.L.; Investigation, L.B., T.Z., K.J.T., N.E.-d., M.A.L. and H.B.; Resources, L.B., T.Z. and K.J.T.; Data curation, L.B., T.Z., N.E.-d., M.A.L., H.B., M.Y.K. and M.M.; Writing—original draft, L.B.; Writing—review & editing, T.Z., K.J.T., N.E.-d., M.A.L., H.B., M.Y.K. and M.M.; Visualization, L.B., T.Z., N.E.-d. and M.A.L.; Supervision, L.B.; Project administration, L.B.; Funding acquisition, L.B. and K.J.T. All authors have read and agreed to the published version of the manuscript.

Funding: This research was funded by a NASA Grant via ROSES solicitation number NNH21ZDA001N, grant number 21-LCLUC21_2-0001 and The APC was funded by the same grant.

Data Availability Statement: Some data from this study are available on request from the authors.

Conflicts of Interest: The authors declare no conflict of interest.

References

1. World Bank Group. World Population, Demographic Statistics. Available online: https://data.worldbank.org/indicator/SP.POP.TOTL (accessed on 12 February 2024).
2. Lall, S.V.; Selod, H. *Rural-Urban Migration in Developing Countries: A Survey of Theoretical Predictions and Empirical Findings*; World Bank Publications: Washington, DC, USA, 2006; Volume 3915.
3. OECD; Sahel and West Africa Club. *Africa's Urbanisation Dynamics 2020: Africapolis, Mapping a New Urban Geography*; West African Studies; OECD: Paris, France, 2020. [CrossRef]
4. O'Neill, A. *Morocco: Urbanization from 2013 to 2023*; Statista: New York, NY, USA, 2025. Available online: https://www.statista.com/statistics/455886/urbanization-in-morocco/ (accessed on 20 May 2024).
5. Bounoua, L.; Zhang, P.; Mostovoy, G.; Thome, K.; Masek, J.; Imhoff, M.; Shepherd, M.; Quattrochi, D.; Santanello, J.; Silva, J.; et al. Impact of Urbanization on US Surface Climate. *Environ. Res. Lett.* **2015**, *10*, 084010. [CrossRef]
6. Grimmond, C.S.B. Climate of Cities. In *The Routledge Handbook of Urban Ecology*; Routledge: London, UK, 2010.
7. Imhoff, M.L.; Zhang, P.; Wolfe, R.E.; Bounoua, L. Remote Sensing of the Urban Heat Island Effect across Biomes in the Continental USA. *Remote Sens. Environ.* **2010**, *114*, 504–513. [CrossRef]
8. World Bank Group. *Analysis of Heat Waves and Urban Heat Island Effects in Central European Cities and Implications for Urban Planning*; PDF 151404; World Bank Group: Washington, DC, USA, 2020. Available online: http://documents.worldbank.org/curated/en/740251596528336330/Analysis-of-Heat-Waves-and-Urban-Heat-Island-Effects-in-Central-European-Cities-and-Implications-for-Urban-Planning (accessed on 14 August 2024).
9. Zhang, P.; Imhoff, M.L.; Bounoua, L.; Wolfe, R.E. Exploring the Influence of Impervious Surface Density and Shape on Urban Heat Islands in the Northeast United States Using MODIS and Landsat. *Can. J. Remote Sens.* **2012**, *38*, 441–451.
10. Fathi, N.; Bounoua, L.; Messouli, M. A Satellite Assessment of the Urban Heat Island in Morocco. *Can. J. Remote Sens.* **2019**, *45*, 26–41. [CrossRef]
11. Bahi, H.; Rhinane, H.; Bensalmia, A.; Fehrenbach, U.; Scherer, D. Effects of Urbanization and Seasonal Cycle on the Surface Urban Heat Island Patterns in the Coastal Growing Cities: A Case Study of Casablanca, Morocco. *Remote Sens.* **2016**, *8*, 829. [CrossRef]
12. Burian, S.J.; Shepherd, J.M. Effect of Urbanization on the Diurnal Rainfall Pattern in Houston. *Hydrol. Process.* **2005**, *19*, 1089–1103. [CrossRef]
13. Ohashi, Y.; Kida, H. Effects of Mountains and Urban Areas on Daytime Local-Circulations in the Osaka and Kyoto Regions. *J. Meteorol. Soc. Jpn. Ser. II* **2002**, *80*, 539–560. [CrossRef]
14. Gong, P.; Li, X.; Wang, J.; Bai, Y.; Chen, B.; Hu, T.; Liu, X.; Xu, B.; Yang, J.; Zhang, W.; et al. Annual Maps of Global Artificial Impervious Area (GAIA) between 1985 and 2018. *Remote Sens. Environ.* **2020**, *236*, 111510. [CrossRef]
15. Marconcini, M.; Metz-Marconcini, A.; Üreyen, S.; Palacios-Lopez, D.; Hanke, W.; Bachofer, F.; Zeidler, J.; Esch, T.; Gorelick, N.; Kakarla, A.; et al. Outlining Where Humans Live, the World Settlement Footprint 2015. *Sci. Data* **2020**, *7*, 242. [CrossRef] [PubMed]

16. Marconcini, M.; Metz- Marconcini, A.; Esch, T.; Gorelick, N. Understanding Current Trends in Global Urbanisation—The World Settlement Footprint Suite. *GI_Forum* **2021**, *1*, 33–38. [CrossRef]
17. Chen, F.; Kusaka, H.; Bornstein, R.; Ching, J.; Grimmond, C.S.B.; Grossman-Clarke, S.; Loridan, T.; Manning, K.; Martilli, A.; Miao, S.; et al. The Integrated WRF/Urban Modeling System: Development, Evaluation, and Applications to Urban Environmental Problems. In *Mechanical and Materials Engineering Faculty Publications and Presentations*; Portland State University: Portland, OR, USA, 2011.
18. Li, H.; Zhou, Y.; Wang, X.; Zhou, X.; Zhang, H.; Sodoudi, S. Quantifying Urban Heat Island Intensity and Its Physical Mechanism Using WRF/UCM. *Sci. Total Environ.* **2019**, *650*, 3110–3119. [CrossRef] [PubMed]
19. Li, H.; Yuan, F.; Shen, L.; Liu, Y.; Zheng, Z.; Zhou, X. Improving the WRF/Urban Modeling System in China by Developing a National Urban Dataset. *Geosci. Front.* **2022**, *13*, 101385. [CrossRef]
20. Tewari, M. Implementation and Verification of the Unified Noah Land Surface Model in the WRF Model. In Proceedings of the 20th Conference on Weather Analysis and Forecasting/16th Conference on Numerical Weather Prediction, Seattle, WA, USA, 12–16 January 2004.
21. Kusaka, H.; Crook, A.; Dudhia, J.; Wada, K. Comparison of the WRF and MM5 Models for Simulation of Heavy Rainfall along the Baiu Front. *SOLA* **2005**, *1*, 197–200. [CrossRef]
22. Skamarock, W.C.; Klemp, J.B.; Dudhia, J.; Gill, D.O.; Barker, D.M.; Duda, M.G.; Huang, X.-Y.; Wang, W.; Powers, J.G. *A Description of the Advanced Research WRF Version 3*; University Corporation for Atmospheric Research: Boulder, CO, USA, 2008.
23. Oke, T.R. The Energetic Basis of the Urban Heat Island. *Q. J. R. Meteorol. Soc.* **1982**, *108*, 1–24. [CrossRef]
24. Quattrochi, D.A. High Spatial Resolution Thermal Infrared Remote Sensing Data for Analysis of the Atlanta, Georgia, Urban Heat Island Effect and Its Impacts on the Environment. 2007. Available online: https://ntrs.nasa.gov/citations/20070032705 (accessed on 12 February 2024).
25. Yanai, M.; Esbensen, S.; Chu, J.-H. Determination of Bulk Properties of Tropical Cloud Clusters from Large-Scale Heat and Moisture Budgets. *J. Atmos. Sci.* **1973**, *30*, 611–627.
26. Landsberg, H.E. *The Urban Climate*; Academic Press: Cambridge, MA, USA, 1981.
27. Kabisch, N.; Remahne, F.; Ilsemann, C.; Fricke, L. The Urban Heat Island under Extreme Heat Conditions: A Case Study of Hannover, Germany. *Sci. Rep.* **2023**, *13*, 23017. [CrossRef] [PubMed]
28. Shepherd, M.J. Making Rain: Do Cities Impact Precipitation? *Weatherwise* **2005**, *58*, 28–31. [CrossRef]
29. Wang, Q.; Zhang, C.; Ren, C.; Hang, J.; Li, Y. Urban Heat Island Circulations over the Beijing-Tianjin Region under Calm and Fair Conditions. *Build. Environ.* **2020**, *180*, 107063. [CrossRef]
30. Zhao, L.; Lee, X.; Smith, M. The effect of urbanization on the spatial distribution of the UHI effect. *Urban Clim.* **2019**, *28*, 100452.